PHYSICAL REVIEW B VOLUME 27, NUMBER 2 15 JANUARY 1983

# Current image diffraction patterns of metal single-crystal surfaces

A. N. Jette, B. H. Nall, and C. B. Bargeron
*Milton S. Eisenhower Research Center, Applied Physics Laboratory, The Johns Hopkins University, Johns Hopkins Road, Laurel, Maryland 20707*
(Received 6 July 1982; revised manuscript received 16 September 1982)

Diffraction patterns in the specimen current images at low electron beam energies of the (100), (110), and (111) surfaces of aluminum and the (100) surface of copper are presented along with theoretical computations for the aluminum (100) surface. With the use of computer imaging techniques, a two-dimensional diffraction pattern for the (100) face of aluminum is generated based on a dynamical calculation of the reflectivity, as a function of the polar and azimuthal angles of the incident electron beam, due to the elastically backscattered electrons. This pattern reproduces the overall experimental features leading to the conclusion that the diffraction patterns are due to the elastically backscattered electrons.

## INTRODUCTION

Recently, diffraction patterns in the specimen current images of (100) and (110) surfaces of single crystals of aluminum were reported.[1] The crystal surfaces were imaged by scanning with low-energy electrons (40—400 eV) and displaying the current absorbed in the specimen synchronously on a cathode ray tube (CRT). The absorbed current depends on the angle of incidence of the primary electron beam, and areas of high reflectivity are revealed by a drop in specimen current corresponding to dark areas in the two-dimensional diffraction pattern. The diffraction patterns displayed in this manner have the characteristic symmetry of the corresponding crystal surfaces and are found to be quite sensitive to surface condition. These patterns are also very dependent on the energy of the electron beam, changing rapidly as the beam energy is varied.

On the basis of a theoretical calculation of the surface reflectivity along two high-symmetry axes of the crystal surface and along an axis midway between, the diffraction phenomena were attributed to the elastically backscattered electrons that are responsible for the low-energy electron-diffraction (LEED) spots. Previous workers[2–4] have observed peaks in total electron yield curves as a function of angle of incidence in the complementary experiment to ours. (We measure total absorbed electron current as opposed to the total emitted electron current.) Most of this work was done at higher energy ($>1$ keV) and involved large variations in angle of incidence ($\sim 60°$). Such peaks are likely due to inelastic processes such as channeling patterns.[5,6] Soshea and Dekker[3] reported total electron yield peaks below 1 keV for titanium single crystals and found only a peak at 0°. At higher energies ($>1$ keV), they found several maxima superimposed on a general increase of electron emission with angle of incidence. Our patterns, on the other hand, are restricted to smaller angles of incidence ($\pm 18°$) and show significant variation with energy at low beam energies ($<400$ eV).

The purpose of this paper is to report further experimental and theoretical investigations into current image diffraction (CID) presenting new experimental data for the (111) aluminum and (100) copper surfaces and additional data for the (100) and (110) aluminum surfaces. The results of a detailed theoretical calculation of the reflectivity of the (100) surface due to the elastically backscattered electrons as a function of the polar and azimuthal angles of the incident electron beam are presented for an energy of 6.55 hartree (1 hartree=27.2 eV) relative to the muffin tin. With these data a computer-developed image of the diffraction pattern on the crystal surface was created and compared with several experimental patterns at various primary beam energies near 6.55 hartree. The resulting correlation between theory and experiment leaves little doubt that the patterns on aluminum are the result of the elastically backscattered electrons in this energy range.

## EXPERIMENT

{100}, {110}, and {111} aluminum and {100} copper single crystals were obtained from the Atomergic Chemetals Corporation. All crystals were of 99.999% purity, about 12.7 mm in diameter, (2—3)-mm thick, and oriented within 1° of their respective surfaces. The surface preparation consisted of a mechanical and an electropolish. For aluminum the electropolish was done in a 10% perchloric

 

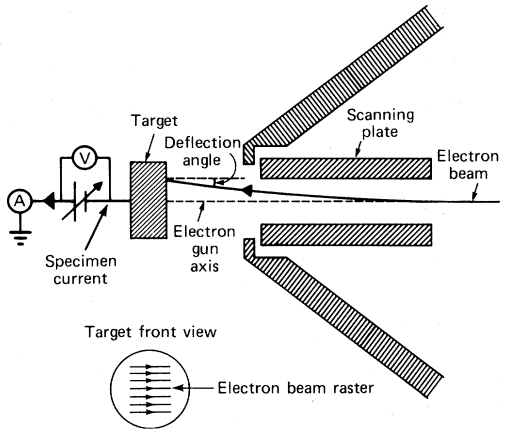


FIG. 1. Schematic diagram of the experimental apparatus.

acid in ethanol mixture at −20 °C as described previously.[7,8] The electropolishing solution for copper was chromic acid in water (200 g/liter). The result in each case was a bright, smooth, though not uniformly flat, surface.

The experimental configuration is illustrated in Fig. 1. The sample surface is imaged by collecting the specimen current and displaying it on a CRT. The actual apparatus is a Physical Electronics Model 545M scanning Auger spectrometer. Owing to the geometry of the deflection plates and their position with respect to the crystal surface, the maximum polar-angle deflection is about ±18°. At beam energies below 150 eV, contrast was improved by applying a negative potential bias to the sample relative to the spectrometer. The beam current was of the order of $10^{-2}$ μA. The Auger spectrometer is also equipped with an ion gun for sputter cleaning and a LEED accessory. Throughout the experiments the base pressure of the system was maintained at $(1-2)\times10^{-10}$ Torr.

After a preliminary bakeout the samples were subjected to a few cycles of sputter cleaning [5—10 min at $4\times10^{-5}$ Torr (Ar) with ion-gun settings of 1 kV and 25 mA] and heating (about an hour at 350 °C). Auger spectroscopy of a cleaned aluminum surface indicated only the metallic Al line with no

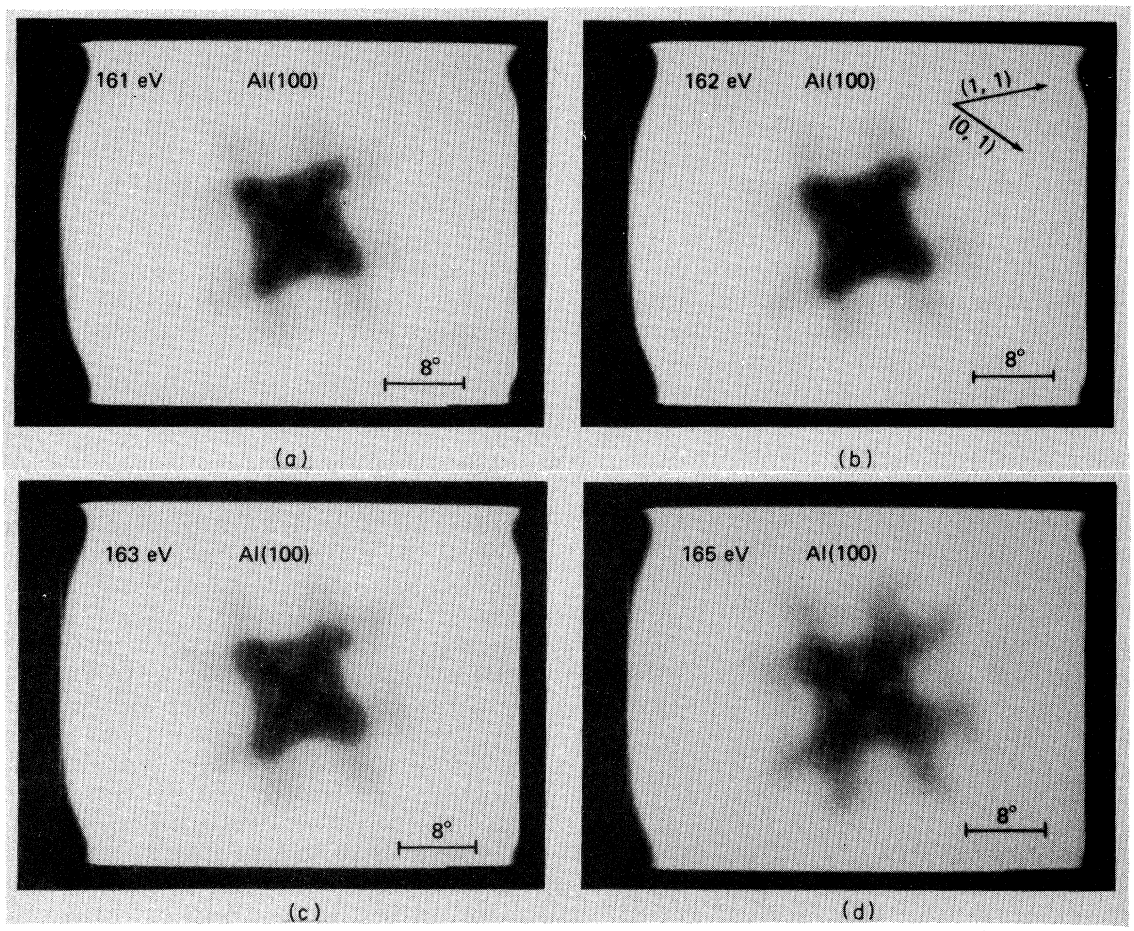


FIG. 2. CID patterns for the (100) face of aluminum for primary beam energies of (a) 161 eV, (b) 162 eV, (c) 163 eV, and (d) 165 eV relative to the sample.

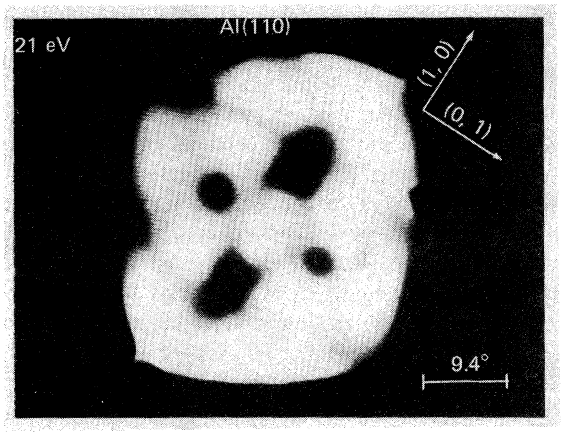


FIG. 3. CID pattern on the (110) face of aluminum at a primary beam energy of 21 eV relative to the sample.

other elements such as oxygen, carbon, or argon. On the cleaned copper crystal the metallic copper lines were observed along with a small sulfur peak shifted to about 130 eV. The surface orientation apparent in the CID patterns was verified with LEED. The LEED spots were bright with low background indicating surfaces of good quality.

In Fig. 2 the dependence of the CID patterns on small variations in energy is demonstrated. The primary beam energy was varied from 161 eV for Fig. 2(a) to 165 eV relative to the sample in Fig. 2(d) (−20 V bias applied in each case). These CID patterns were obtained from the (100) face of aluminum, and the crystal symmetry of this face is apparent in the patterns. A CID pattern on the (110) face of aluminum appears in Fig. 3 for an energy of 21 eV (−50 V bias). The hexagonal symmetry of the (111) face of aluminum is evident in the CID pattern for an energy of 31 eV (−39 V bias) in Fig. 4. Finally, in Fig. 5 a CID pattern on the (100) face of copper is shown for a primary beam energy of 30

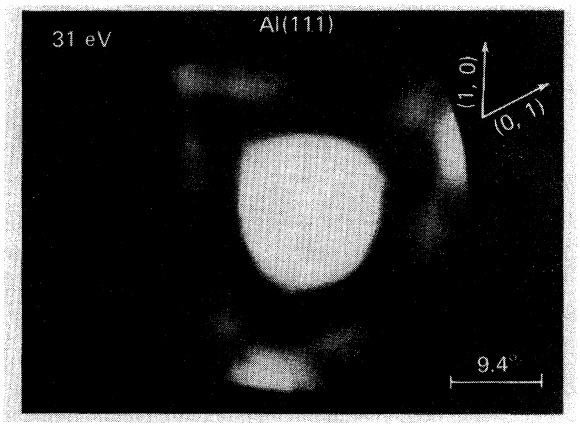


FIG. 4. CID pattern on the (111) face of aluminum at a primary beam energy of 31 eV relative to the sample.

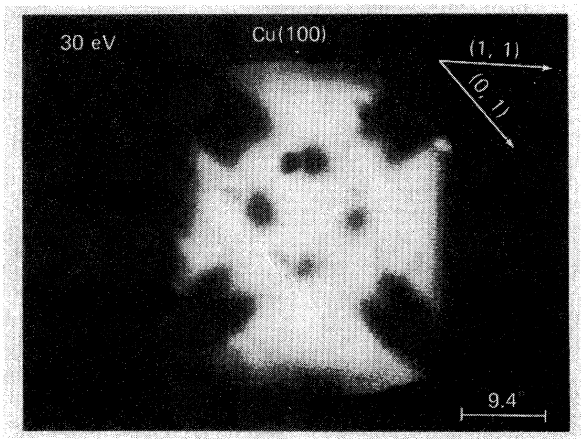


FIG. 5. CID pattern on the (100) face of copper at a primary beam energy of 30 eV relative to the sample.

eV (−45 V bias). On all of these faces the CID patterns reveal the crystal orientation as verified with LEED and are quite sensitive to primary beam energies. The fact that image contrast is increased by the application of a negative potential to the sample relative to nearby parts of the spectrometer is an indication that low-energy secondary electrons make a contribution to the contrast. Soshea and Dekker[3] measured the energy distribution of the electrons emitted from the (0001) surface of titanium and determined for a 520-eV beam at normal incidence that 36% of the peak in the electron yield was due to backscattered primary electrons. They also attributed the increase in lower-energy secondaries at near-normal incidence to diffracted beams traveling at large angles to the normal which create more secondaries near the surface from where they can escape.

## THEORY

The intensity of elastically backscattered electrons as a function of polar and aximuthal angles and primary beam energy was computed using the renormalized forward scattering perturbation theory[9] and the computer codes in the appendix of Pendry's book.[10] In this theory the ion cores, arranged in layers parallel to the surface, are immersed in a constant complex potential (optical potential) and both intralayer and interlayer multiple-scattering effects are considered with the strong interlayer forward scattering being included to all orders while perturbation theory is used to treat the weak backscattering. The beams are attenuated by the imaginary component of the optical potential taken as −5.44 eV. Eight phase shifts and 49 beams were included in the computation and temperature effects were excluded. The results of this computation for the (100) surface of aluminum are plotted in Figs. 6 and

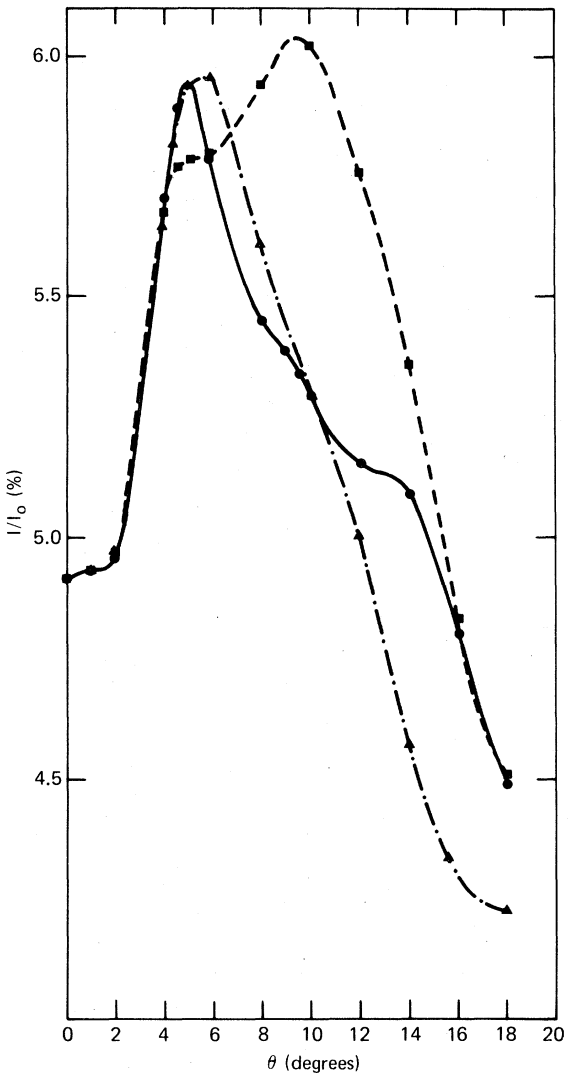


FIG. 6. Theoretical elastic backscattered electron current for Al(100) as a function of angle of incidence along the (1,1) direction ——●——, the (1,0) direction of the reciprocal lattice —·—▲—·—, and midway between --■--. The primary beam energy is 6.69 hartree relative to the muffin tin.

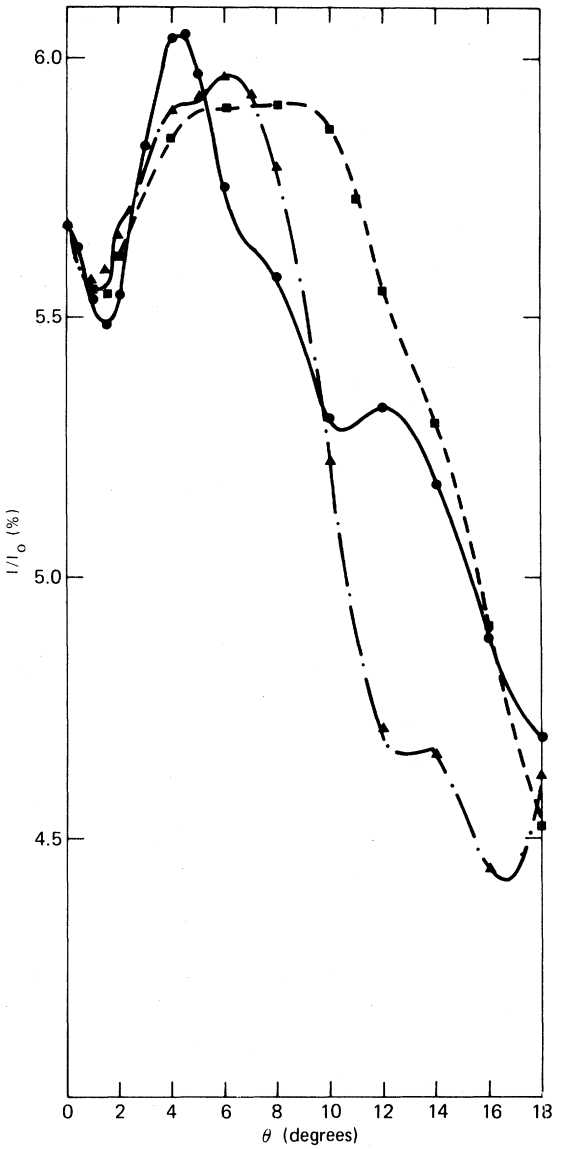


FIG. 7. Theoretical elastic backscattered electron current for Al(100) as a function of angle of incidence along the (1,1) direction ——●——, the (1,0) direction of the reciprocal lattice —·—▲—·—, and midway between --■--. The primary beam energy is 6.55 hartree relative to the muffin tin.

7 for primary beam energies of 6.69 and 6.55 hartree relative to the muffin tin, respectively. In these figures the total percentage of electrons elastically backscattered along the high-symmetry (1,0) and (1,1) axes of the reciprocal lattice are shown along with a direction midway between these axes. It was found that small changes in the primary beam energy (1 eV) induces observable effects in the theoretical curves as had been observed experimentally (Figs. 2).

No one LEED beam is responsible for these angular variations in contrast across the surface of the crystal as indicated in Fig. 8, where the intensity variations are shown of all the LEED beams that can backscatter from the crystal at a primary beam energy of 6.55 hartree for angles of incidence from 0 to 18° along the (1,1) direction of the reciprocal lattice. It is noted that the (3,0) and (0,3) beams become evanescent at 3° as does the (2,2) beam at 4.5°. Furthermore, as the angle of incidence increases, new beams appear; namely, the sets $(\bar{1},\bar{3})$ and $(\bar{3},\bar{1})$ at 1.5°, $(\bar{3},1)$ and $(1,\bar{3})$ at 3°, and $(\bar{2},\bar{3})$ and $(\bar{3},\bar{2})$ at 8.5°. Thus, as the angle of incidence increases, some

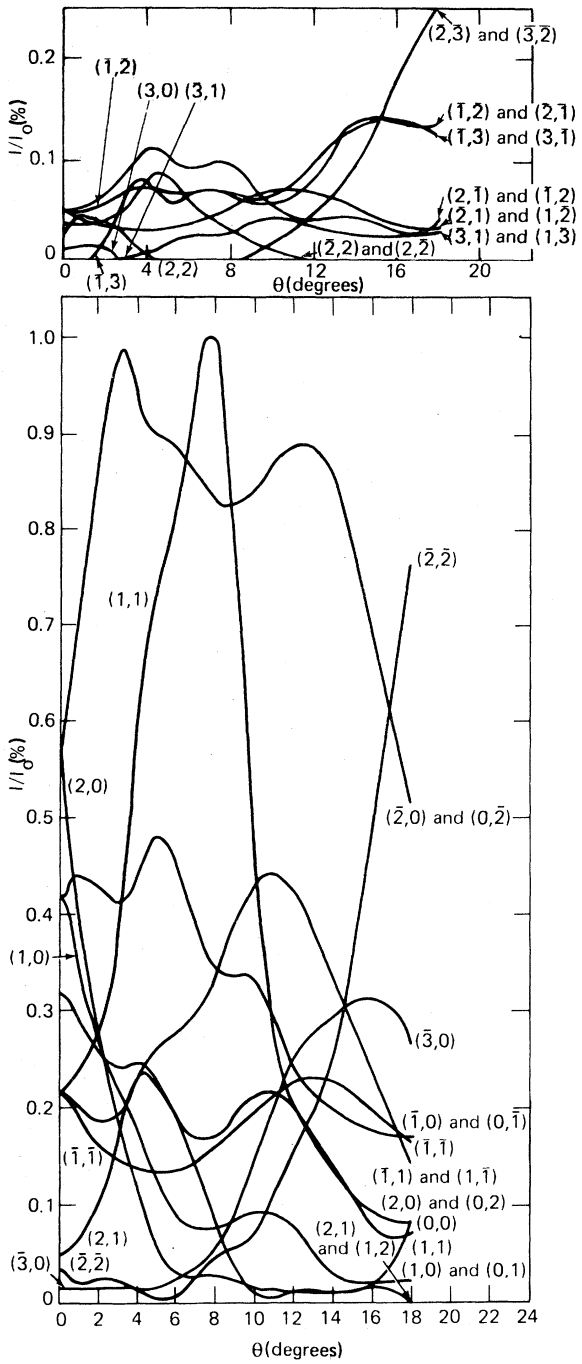


FIG. 8. Theoretical intensity variations of individual LEED beams as a function of angle of incidence along the (1,1) axis of the reciprocal lattice of Al(100) for a primary beam energy of 6.55 hartree.

of the LEED beams disappear, as they can no longer leave the crystal, and new ones appear. It is important to include enough beams in calculations to take this effect into account. From Fig. 8 it is also apparent that the maximum at the 0° angle of incidence in Fig. 7 is primarily due to the sharp drop in intensity of the (0,1) and (1,0) beams as $\theta$ increases.

In order to facilitate the comparison of theory and experiment, the total reflectivity was calculated as a function of angle of incidence of the primary beam, using a dynamical theory,[9] at 130 points forming a grid in one octant of the (100) surface of aluminum. These calculations were for a beam energy of 6.55 hartree relative to the muffin tin. The points in this octant were interpolated using cubic spline functions to a total of 1250 points for the octant. Assuming a linear-response function and using computer imaging methods, the theoretical diffraction pattern displayed in Fig. 9 was created. The contrast in this generated image has been reversed so that bright areas in Fig. 9 correspond to low reflectivities (i.e., correspond to the experimental measurements). This pattern bears a marked resemblance to those of Fig. 2, particularly Fig. 2(c), which would correspond to an inner potential of 15 eV. The primary discrepancy between theory and experimental is the large dark spot at the center ($\theta = 0°$) which theory predicts should be much smaller and weaker (Figs. 7 and 9). It should be borne in mind that temperature effects were ignored in the theory, that the experiment was done at room temperature using an energy-broadened electron beam, and that theory neglects a nonlinear image enhancement as a function of beam angle of incidence due to secondary electron emission via the diffracted-beam mechanism[3] mentioned above. (It should be noted that the low-energy secondary electron current is on the order of 10 times greater than the elastically backscattered current at this beam energy. Therefore, non-

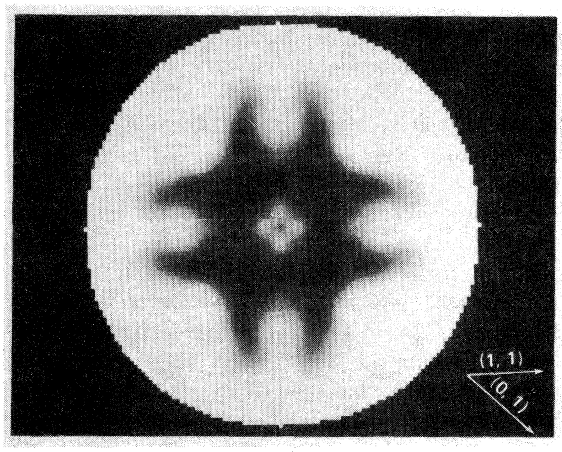


FIG. 9. Theoretical image on the (100) aluminum surface for a primary beam energy of 6.55 hartree relative to the muffin tin. High reflectivity is indicated by dark areas and directions are shown along the reciprocal lattice.

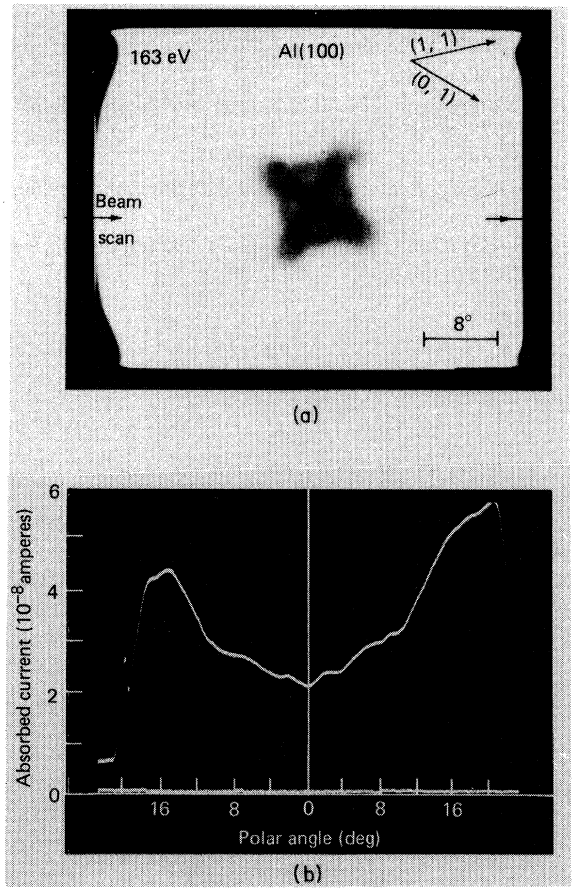


FIG. 10. Electron absorption as a function of angle of incidence on the (100) surface of aluminum at a primary beam energy of 163 eV relative to the vacuum. (a) CID pattern showing line of beam scan and (b) electron absorption along line of beam scan. The beam current was $1.9\times10^{-7}$ A for the line scan.

linear enhancement could be substantial.) This would explain the much sharper features appearing in the theoretical image than those observed in the experimental picture. Nevertheless, the overall features apparent in the experimental picture are in the theoretical image, leading us to conclude that the images are due to the elastically backscattered electrons.

## DISCUSSION

The electron current absorbed as the beam sweeps across the crystal is shown in Fig. 10(b), where the arrows in the CID pattern of Fig. 10(a) indicate the direction and position of the beam scan. The asymmetry with respect to normal incidence, $\theta=0°$, apparent in Fig. 10(b) is due to an experimental artifact involving the crystal holder. This curve is quite interesting since it indicates a maximum of reflectivity at 0° and a decrease in reflectivity or increase in absorbed current as the polar angle increases. This is precisely what Soshea and Dekker[3] observed for the total electron yield from the (0001) surface of titanium over this angular range ($\pm18°$) and low energy ($<1$ kV). But, also superimposed on this increase in absorbed current with polar angle is a modulation or fine structure which is responsible for the CID patterns. Soshea and Dekker observed this same phonemenon (what they termed ultrahigh fine structure) on the total electron yield peaks for primary beam energies over 1 kV which they attributed to electron diffraction (probably electron channeling patterns which had not yet been discovered and explained[5,6]). They found significant scatter in their data at low energies, however, and one can only speculate that this might have also been due to the diffraction process responsible for the CID patterns.

Information on crystal orientation and structure can obviously be obtained from the CID patterns. However, whether this method can give quantitative structural information such as LEED and surface-extended x-ray-absorption fine structure (SEXAFS), is still in an exploratory stage. Changes in the CID patterns on the aluminum (111) surface have been seen upon oxygen adsorption,[11] but much work remains to be done in developing this method as a tool for surface analysis.

## CONCLUSION

In this paper we have presented additional experimental data of CID patterns on aluminum surfaces and have shown that the effect can also be observed on copper. These data indicate the sensitivity of the patterns to primary beam energy, crystal structure, and orientation. Theoretical calculations were presented that also corroborate these observations. Finally, an image of the crystal due to elastically backscattered electrons based on the theoretical computations was obtained using computer imaging techniques, confirming our conclusion that at least on the aluminum surfaces, at low beam energies, the CID patterns are the result of elastic diffraction processes.

## ACKNOWLEDGMENTS

The authors wish to acknowledge helpful discussions with Dr. S. N. Foner, the technical assistance of Mr. R. B. Givens, and the computing support of Mr. S. Favin. This work was supported by the Naval Sea Systems Command, U.S. Department of the Navy, under Contract No. N00024-81-C-5301.

[1]B. H. Nall, A. N. Jette, and C. B. Bargeron, Phys. Rev. Lett. 48, 882 (1982).
[2]A. B. Laponsky and N. Rey Whetten, Phys. Rev. Lett. 3, 510 (1959).
[3]R. W. Soshea and A. J. Dekker, Phys. Rev. 121, 1362 (1961).
[4]R. M. Stern and H. Taub, Phys. Rev. Lett. 20, 1340 (1968).
[5]D. G. Coates, Philos. Mag. 16, 1179 (1967).
[6]G. R. Booker, A. M. B. Shaw, M. J. Whelan, and P. B. Hirsch, Philos. Mag. 16, 1185 (1967).
[7]B. H. Nall, A. N. Jette, and C. B. Bargeron, Surf. Sci. 110, L606 (1981).
[8]J. K. Grepstad, P. O. Gartland, and B. J. Slagsvold, Surf. Sci. 57, 348 (1976).
[9]J. B. Pendry, J. Phys. C 4, 3095 (1971).
[10]J. B. Pendry, *Low Energy Electron Diffraction* (Academic, London, 1974).
[11]C. B. Bargeron, B. H. Nall, and A. N. Jette, Surf. Sci. 120, L483 (1982).

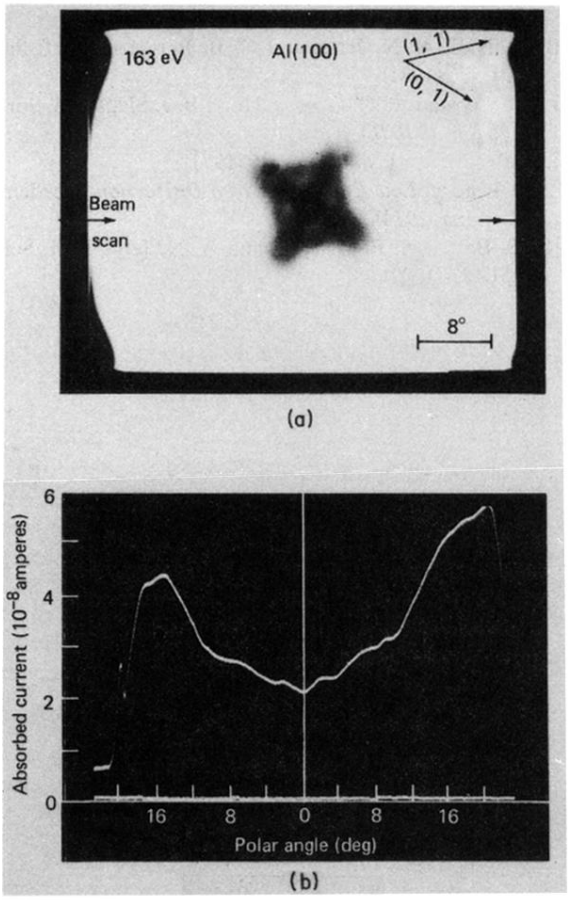


FIG. 10. Electron absorption as a function of angle of incidence on the (100) surface of aluminum at a primary beam energy of 163 eV relative to the vacuum. (a) CID pattern showing line of beam scan and (b) electron absorption along line of beam scan. The beam current was $1.9\times10^{-7}$ A for the line scan.

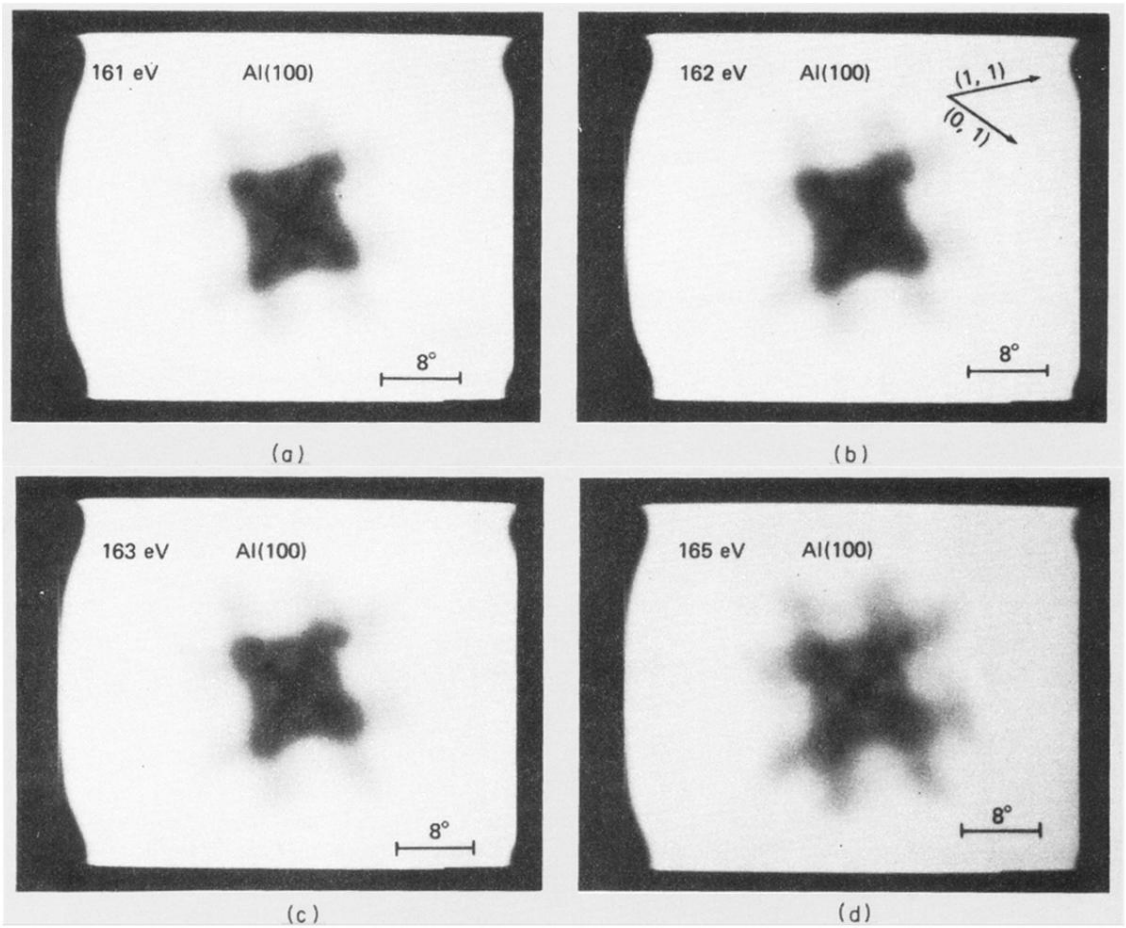


FIG. 2. CID patterns for the (100) face of aluminum for primary beam energies of (a) 161 eV, (b) 162 eV, (c) 163 eV, and (d) 165 eV relative to the sample.

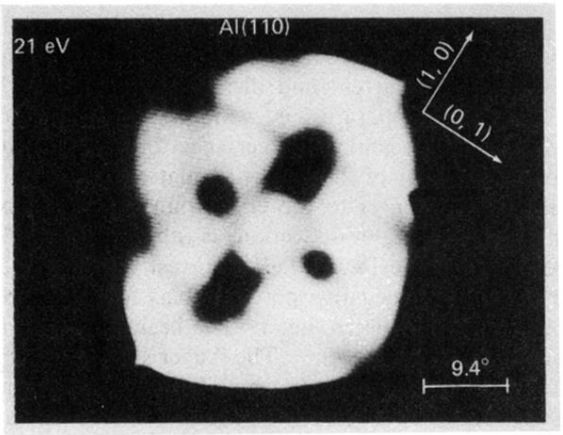


FIG. 3. CID pattern on the (110) face of aluminum at a primary beam energy of 21 eV relative to the sample.

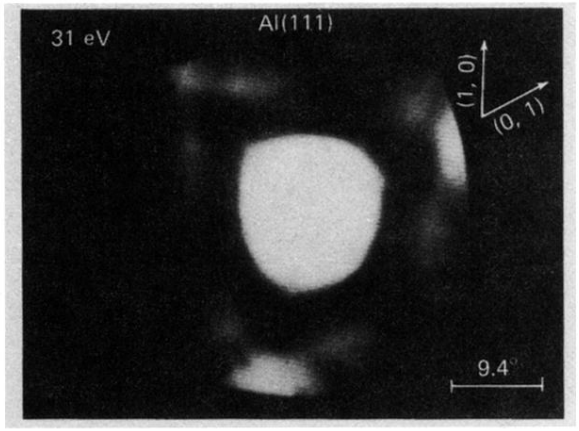


FIG. 4. CID pattern on the (111) face of aluminum at a primary beam energy of 31 eV relative to the sample.

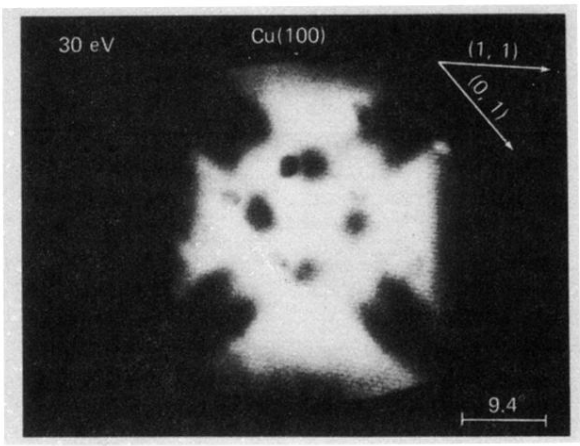


FIG. 5. CID pattern on the (100) face of copper at a primary beam energy of 30 eV relative to the sample.

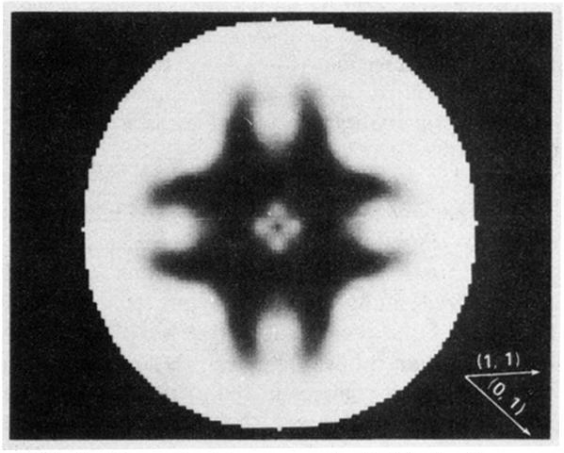


FIG. 9. Theoretical image on the (100) aluminum surface for a primary beam energy of 6.55 hartree relative to the muffin tin. High reflectivity is indicated by dark areas and directions are shown along the reciprocal lattice.